Structure and Energetics of Water−Silanol Binding on the Surface of Silicalite-1: Quantum Chemical Calculations

O. Saengsawang,[†] T. Remsungnen,[‡] S. Fritzsche,[§] R. Haberlandt,[§] and S. Hannongbua*,[†]

Department of Chemistry, Faculty of Science, Chulalongkorn University, Bangkok 10330, Thailand, Department of Mathematics, Faculty of Science, Khon Kean University, Khon Kaen 40002, Thailand, and Department of Molecular Dynamics/Computer Simulation, Faculty of Physics and Geoscience, Institute for Theoretical Physics (ITP), University of Leipzig, Augustplatz 0-11, 04109 Leipzig, Germany

Quantum mechanical calculations have been carried out to investigate the structural properties and the interaction between water molecules and silanol groups on the surface of silicalite-1. The (010) surface, which is perpendicular to the straight channel, has been selected and represented by three fragments taken from different parts of the surface. Calculations have been performed using different levels of accuracy: HF/6-31G(d,p), B3LYP/6-31G(d,p), HF/6-31++G(d,p), and B3LYP/6-31++G(d,p). The basis set superposition error has been taken into account. The geometry of the silanol groups and that of the water molecules have been fully optimized. The results show that the most stable conformation takes place when a water molecule forms two hydrogen bonds with two silanols, with only one silanol lying on the opening of the pore of the straight channel. The corresponding binding energy is −48.82 kJ/mol. These areas are supposed to be the first binding sites which have to be covered when the water molecule approaches the surface. When the water loading increases, the next favorable silanols are those of the opening of the pore in which the four possible complex conformations yield a binding energy between −25.62 and −37.41 kJ/mol. It was also found that the calculated O−H bond length of the silanol in the free form was slightly shorter than that in the complex. In terms of the stretching frequency, the complexation leads to a red shift of the O−H stretching of the silanol group.

Introduction

Zeolites are microporous aluminosilicate materials which have numerous properties that are appropriate for catalysis and separation. The high porosity and the regular system of nanosize pores lead to beneficial characteristics of these materials, for example, shape selectivity and catalytic properties. However, before the guest molecules may get into the region of activity within the pore system, they have to diffuse through the pore opening, which means they have to interact with the external surface. Only recently,[1−3] approaches of guest molecules and penetration through the zeolite surface have become a subject of investigation. Experimental evidence exists which shows the significant role of external and internal surfaces and the very complicated nature of their interplay in the shape selective catalysis. Turro and co-workers used a combination of different spectroscopic techniques to show the very complicated nature of shape selective catalysis in photolysis reactions of many ketone molecules by FAU and MFI as caused by the external and internal surface.[4,5] Isomerization of 1,2,4-trimethylbenzene over zeolite NU-87 was observed to take place mainly on the external surface,[6] while alkylation of biphenyl over various zeolites was observed only on the external surfaces.[7,8] The external surface also contributes to the adsorption of C_6−C_9 *n*-alkanes on Pt/H-ZSM-22.[9]

It is known that the key elements determining the adsorption and diffusion behavior of guest molecules on the external surfaces are silanol groups. Most of the information on the characteristics of silanol on the external surface of zeolites arises from Fourier transform infrared (FTIR) experiments.[10] It was found that the surface of most of the zeolitic and amorphous silica materials is covered by silanol groups.

Noncationic zeolites, in particular, silicalite-1, are widely used in the separation of mixtures of light hydrocarbons with water or other polar solvents. It should be noted that the internal surface of perfect silicalite-1 is hydrophobic, whereas the external surface is hydrophilic. This can be attributed to terminal silanol groups which are able to interact with guest molecules. Several FTIR experiments disclose that the O−H bond of silanol groups is softened when interacting with nitriles,[11−14] alcohols,[15] water,[16] pyridine,[17] and even aliphatic and aromatic hydrocarbons.[13] However, most of the experimental and theoretical works focus on the internal surface, which means the pore or channel, whereas much less is known about the details of the external surface.

In this study, the interaction between the silanol groups on the external surface of silicalite-1 and water molecules has been investigated. The energetic and geometric optimizations have been performed using quantum chemical calculations at the Hartree−Fock (HF) and density functional theory (DFT) levels. In addition, the calculated vibrational frequencies have been evaluated and compared with the experimental data.

Theoretical Calculations

Naked Cluster Models. The (010) surface of the silicalite-1, which is perpendicular to the straight channels, was selected and cut from the idealized lattice of MFI using the Cerius2

* Corresponding author. E-mail: supot.h@chula.ac.th.
† Chulalongkorn University.
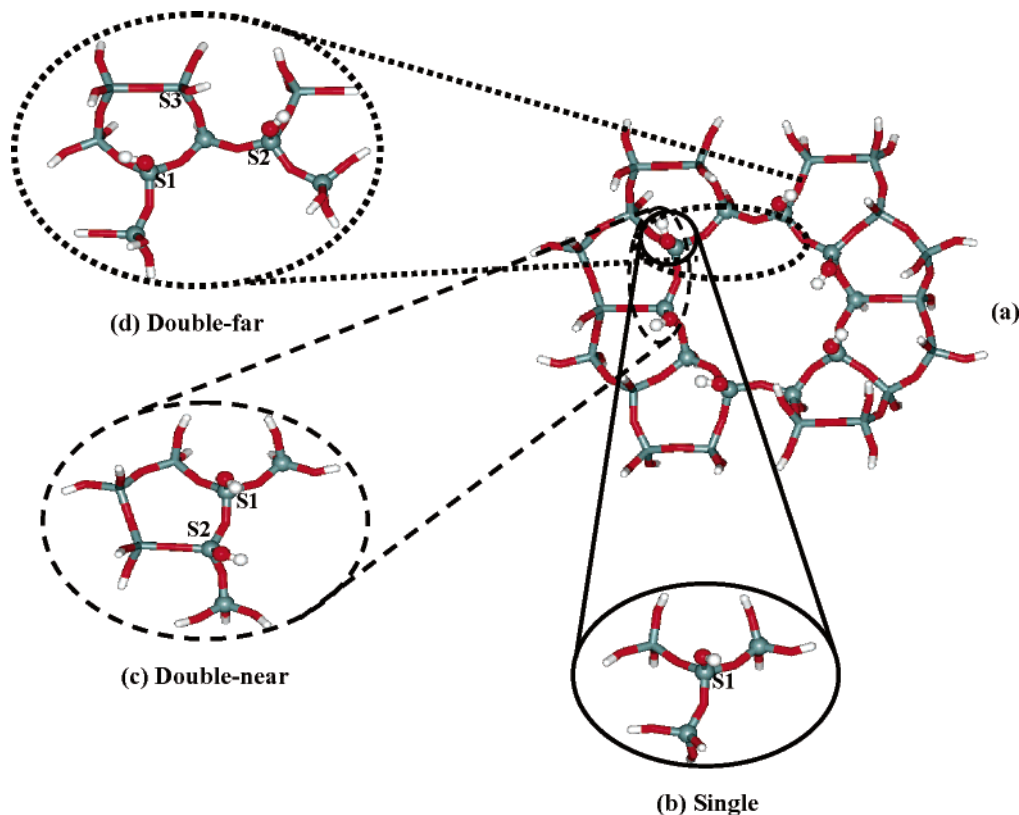‡ Khon Kean University.
§ University of Leipzig.

Figure 1. The (010) surface of silicalite-1 (a) and the three $Si_4O_{13}H_{10}$ (b), $Si_7O_{22}H_{16}$ (c), and $Si_9O_{27}H_{18}$ (d) clusters, used to represent the surface in the quantum chemical calculations to evaluate interactions between water molecules and single (S1), double-near and double-far silanol groups (S1 and S2), respectively (for details, see text).
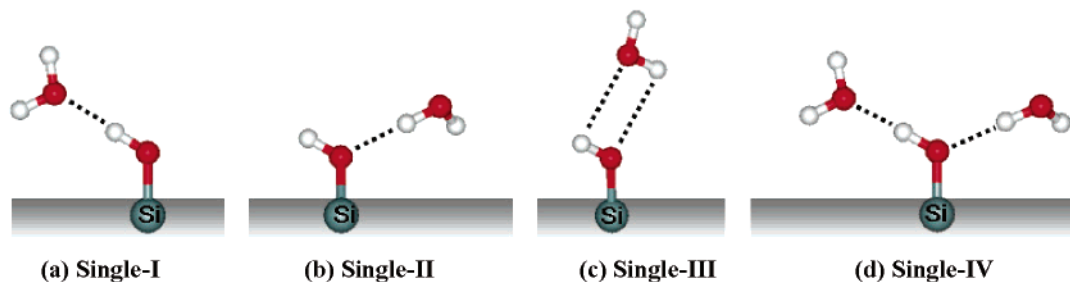

Figure 2. Four investigated conformations representing the interaction between a single silanol and one water molecule (a–c) or two water molecules (d).

program. Silanol groups on the surface were generated by adding hydrogen atoms to the broken O–Si bonds. However, the obtained fragment is still too large for the high level quantum chemical calculations. Therefore, the silanol group models were represented by three clusters taken from different parts of the (010) surface. They were named, for simplification, as single silanol (Figure 1b, single), double silanol bridged by an −O− group (Figure 1c, double-near), and double silanol bridged by an −O−Si−O− group (Figure 1d, double-far). They were respectively used to model interactions with the isolated (single) silanol and two possible configurations of the two (double) contacted silanols on the (010) surface. The hydrogen atoms were added to SiO− groups of the selected fragment, by replacing silicon atoms of the lattice. All O–H bond lengths and Si–O–H angles as well as the rotation of isolated silanol groups around the Si–O bond were optimized, using different levels of quantum chemical calculations. The chemical compositions of the selected single, double-near, and double-far fragments, after filling up the remaining valence orbitals of the oxygen atoms by hydrogen atoms, are $Si_4O_{13}H_{10}$, $Si_7O_{22}H_{16}$, and $Si_9O_{27}H_{18}$, respectively.

Geometries, Interaction Energies, and Vibrational Frequencies of the Complexes. Four possible configurations of water molecules were assigned to bind to a single silanol group to form mono- (Figure 2a–c) and dihydrated (Figure 2d) complexes. They are, then, denoted as single-I to single-IV, as shown in Figure 2. For the two contacted silanols bridged by an −O− group (double-near) where the O–O distance between the two silanols is 3.86 Å, three possible binding configurations, double-near-I to double-near-III, as shown in Figure 3a–c, were proposed. The situation is different for the double-far complex where the O–O distance between the two contacted silanols of 5.75 Å is large enough to accommodate two water molecules. Therefore, the two possible complexes shown in Figure 3d and e were examined. Note that the distance between the two silanols in the double-far system is too large to form complexes with water molecules, as in the configurations shown in Figure 3b and c (details are discussed later).

The intramolecular geometries of the water molecule (O–H bonds and H–O–H angle) and of the silanol group (O–H bond) as well as the intermolecular parameters (distances and orientation of water molecules relative to the silanol group) were fully
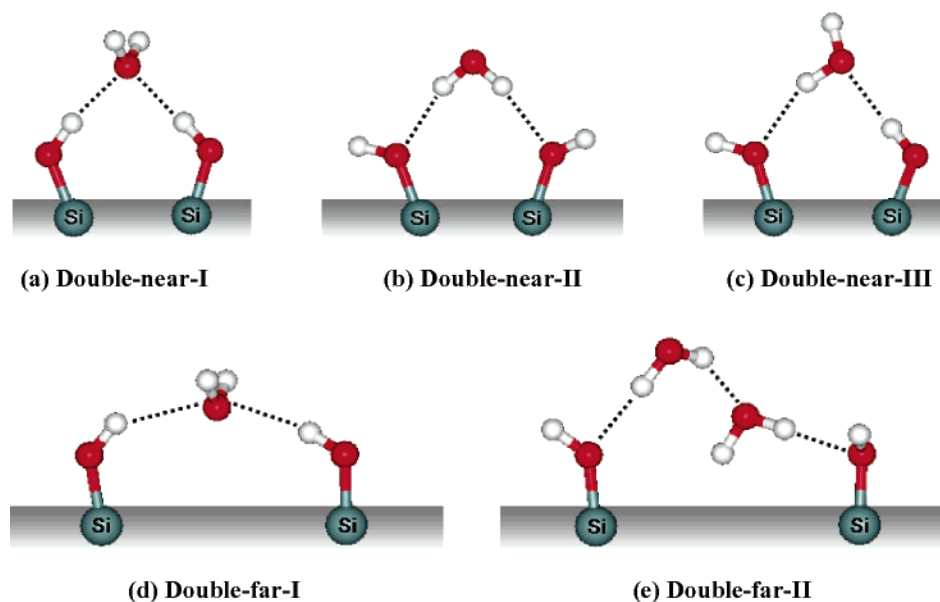
Figure 3. Investigated conformations representing interactions between a water molecule and a double silanol group: double-near (a−c); double-far (d and e).

optimized, using different levels of accuracy. The vibrational frequencies of the water molecule and the silanol group were investigated using the second derivative of the energy with respect to the atomic coordinates in the self-consistent field (SCF) calculations. The results were reported in comparison to the experimental data. Note that scaling factors of 0.89 and 0.96 were applied for the HF and the B3LYP frequency calculations, respectively. In addition, symmetric stretching was assumed in the calculations of the vibrational frequencies of water molecules in the asymmetric complexes shown in Figure 3c and e.

The following two procedures were applied to the quantum chemical calculations. First, the geometry of the complex was optimized using the Hartree−Fock method with the 3-21G* basis set, HF/3-21G*, and then, a single point calculation was performed using different levels of accuracy, HF/6-31G(d,p), HF/6-31++G(d,p), B3LYP/6-31G(d,p), and B3LYP/6-31++G-(d,p), to get the energy and spectroscopic properties of the complexes. Second, the same method and level of accuracy was applied to both steps, namely, geometry optimizations and energies as well as spectroscopic calculations. For simplification, abbreviations were used, for example, HF/3-21G*//HF/6-31++G-(d,p), HF/3-21G* and HF/6-31++G(d,p) were used in the geometry optimization and the single point calculation, respectively.

Binding energies, ΔE_{bind}, for the single silanol cluster are described by the summation of the two terms

$$\Delta E_{bind} = \Delta E_{def} + \Delta E_{int} \quad (1)$$

where ΔE_{def} is the deformation energy required to change the geometries of water and silanol from their equilibrium configuration in free forms, (water-free) and (cluster-free), to those corresponding to the complexed form, (water-cpx) and (cluster-cpx), defined as

for cluster: $\Delta E_{def} = E(cluster\text{-}cpx) - E(cluster\text{-}free)$ (2a)

for water: $\Delta E_{def} = E(water\text{-}cpx) - E(water\text{-}free)$ (2b)

where $E(cluster\text{-}cpx)$ and $E(cluster\text{-}free)$ are the total energies of the clusters in the configuration given in parentheses. The same manner was also applied for $E(water\text{-}cpx)$ and $E(water\text{-}$

free). For the second term in eq 1, ΔE_{int} was defined on the basis of a supermolecular approach according to eq 3:

$$\Delta E_{int} = E(cluster\text{-}cpx/water) - E(cluster\text{-}cpx) -$$
$$E(water\text{-}cpx) \quad (3)$$

Here, $E(cluster\text{-}cpx/water)$ stands for the total energy of the complex in its optimal configuration. The basis set superposition errors (BSSEs) were corrected for all interaction energy calculations. The SCF calculations were carried out using the GAUSS-IAN 98 package.[18]

For the double silanol groups complexed with one or two water molecules, the two silanol clusters have to be rotated to the configuration suitable for complexation. The rotational energy required for this process was included in ΔE_{def}, which is defined in eq 2a.

Results and Discussion

Single Silanol Complexes. With the four selected configurations (Figure 2) and the surface geometry yielded from the HF/3-21G* optimization, the interactions between a water molecule and a single silanol group were calculated using different levels of accuracy. The results show that the stability trend, in terms of either interaction energy or binding energy per water molecule, is in the following order: single-I < single-IV < single-II ≪ single-III.

Some doubts arose when the HF/3-21G* calculation was applied to evaluate the geometry of the complexes, in which the interaction and the deformation energies are configuration dependent. A complication could arise from the variation of the interaction and the deformation energies, and hence the binding energy (see eq 1), obtained from different calculations which amount ranging from −20.90 to −32.48 kJ/mol and 0.29 up to 9.28 kJ/mol, respectively. The reason for such an event can be due to the fact that the optimal geometry of the surface yielding from HF/3-21G* and used for the single point calculation is not the optimal form for the higher level calculations.

To examine the above-mentioned discrepancy, different methods were applied to optimize the geometry of the silanol cluster. The calculated geometry of the single silanol in the free form (Figure 1b) and the corresponding atomic net charges were

Water−Silanol Binding on the Surface of Silicalite-1

J. Phys. Chem. B, Vol. 109, No. 12, 2005 **5687**

TABLE 1: Optimal Geometry, O−H Bond Length (Å) and Si−O−H Bond Angle (deg), and Atomic Net Charges (au), q_i, Where i Denotes H, O, and Si Atoms of the Single Silanol in Free Form Yielded from Different Calculations

parameter	HF/3-21G*	HF/6-31G(d,p)	HF/6-31++G(d,p)	B3LYP/6-31G(d,p)	B3LYP/6-31++G(d,p)
O−H	0.9557	0.9396	0.9399	0.9600	0.9599
∠Si−O−H	130.3	121.5	122.5	119.3	121.4
q_H	0.426	0.362	0.417	0.330	0.398
q_O	−0.778	−0.719	−1.294	−0.568	−1.132
q_{Si}	1.573	1.497	3.454	0.990	2.879

TABLE 2: Interaction and Deformation Energies (kJ/mol) Representing the Complexation between Water and Single Silanol Groups in the Configurations Shown in Figure 2 Where the Surface Optimization and the Energy Calculations Were Performed Using the Same Levels of Accuracy (See Calculation Details)

cluster type	HF/6-31G(d,p)//HF/6-31G(d,p)		HF/6-31++G(d,p)//HF/6-31++G(d,p)		B3LYP/6-31G(d,p)//B3LYP/6-31G(d,p)		B3LYP/6-31++G(d,p)//B3LYP/6-31++G(d,p)	
	$\Delta E_{int}/\Delta E_{def}$	ΔE_{bind}	$\Delta E_{int}/\Delta E_{def}$	ΔE_{bind}	$\Delta E_{int}/\Delta E_{def}$	ΔE_{bind}	$\Delta E_{int}/\Delta E_{def}$	ΔE_{bind}
single-I	−30.64/0.46	−30.18	−27.17/0.21	−26.96	−35.74/2.59	−33.15	−30.60/0.59	−30.01
single-II	−14.17/0.21	−13.96	−14.63/0.08	−14.55	−18.35/1.88	−16.47	−19.27/0.13	−19.14
single-III	−4.47/0.08	−4.39	−4.77/0.04	−4.72	−5.52/1.63	−3.89	−4.81/0.04	−4.77
single-IV[a]	−46.94/0.84	−46.11	−43.39/0.46	−42.93	−58.06/3.55	−54.51	−53.04/1.17	−51.87
		(−23.06)		(−21.46)		(−27.26)		(−25.94)

[a] The binding energy per water molecule is given in parentheses.

given in Table 1. The calculated data support our assumption on the discrepancy in the prediction of the binding energy of the complexes between the single silanol and the water molecule (Figure 2). The O−H bond length ∼0.94 Å as obtained by the HF method is slightly shorter than the value ∼0.96 Å as obtained from the B3LYP calculation. The Si−O−H angle of the silanol group 130.3° resulting from the HF optimization with the small basis set is significantly larger than those between 119 and 123° obtained by the other calculations. In addition, it was also found that the atomic net charges, especially on the O and Si atoms of the silanol, strongly depend on the method and the basis set used.

To overcome the difficulty due to the surface geometry which is not in the optimal configuration for each calculation, the same method and the same level of accuracy were applied to the optimization of the geometry as well as the single point energy calculations. The results are shown in Table 2.

Among the three configurations where one water molecule binds to a single silanol group (Figure 2a−c), the stabilization energies yielded from all models have the same trend, which is single-I < single-II ≪ single-III. On the basis of thermal fluctuation at room temperature, T, that is, $kT \sim 2.51$ kJ/mol, where k denotes Boltzmann's constant, it can be concluded that all models suggest single-I (Figure 2a) and single-IV (Figure 2d) as the preferential conformations for the silanol−water complex. The calculated binding energy is ranging between −21.46 and −33.15 kJ/mol. However, the B3LYP/6-31++G-(d,p) binding energy is proposed to be the optimal value because of the following reasons. (i) The B3LYP method is superior to the HF calculation because the electron correlation was included. (ii) The 6-31++G(d,p) basis set is more reliable than the 6-31G-(d,p) one because the electron diffusion is taken into account. This leads to the conclusion that the two predicted conformations where one water molecule forms a hydrogen bond by pointing the O atom to the silanol (Figure 2a) and two water molecules bind to one silanol in the configuration shown in Figure 2d yielded a binding energy lying in the range −25.94 to −30.01 kJ/mol (Table 2).

In terms of the deformation energy, the data for all models in Table 2 are much lower than those yielded from HF/3-21G*; the maximum value in Table 2, 3.55 kJ/mol, is much lower than the value 9.28 kJ/mol obtained from the HF/3-21G* optimization. This clearly indicates that, in comparison to the conformations resulting from the HF/3-21G* optimization, the equilibrium geometries of the water molecule and the cluster in the free forms, (water-free) and (cluster-free), shown in Table 1 are closer to those suitable for complexation, (water-cpx) and (cluster-cpx), for each level of calculations.

Geometries of Single Silanol Complexes. In Table 3, intra- and intermolecular geometries of water, naked surface, and surface−water complexes in the four configurations shown in Figure 2 were summarized. Here, the same method was used to optimize water, naked surface, and complex geometries.

The water geometries yielded from the four models, HF and B3LYP methods with 6-31G(d,p) and 6-31++G(d,p) basis sets, are in good agreement with the experimental measurements.[19] The Hartree−Fock O−H bond of ∼0.943 Å is slightly shorter than the experimental one, while the B3LYP value ∼0.965 Å is longer than the experimental data. In addition, no significant difference of the O−H bond was found among the two basis sets used. In terms of the H−O−H angle, the B3LYP method is slightly better than the HF method in representing the experimental data (104.48 Å). For the naked (010) surface (Table 3) represented by the $Si_4O_{13}H_{10}$ fragment, as shown in Figure 1b, the predicted O−H bond of the silanol group is in the range 0.94−0.96 Å.

Considering the silanol−water complex, attention was focused to the single-I complex where the most stable conformation of the complex was detected. The experimental O−H bond length of the silanol (0.956−1.000 Å) and the intermolecular distance between oxygen atoms of the silanol and water molecules, $O_s \cdots O_w$ (2.70−2.90 Å), cover broad ranges,[20] including all calculated data. The calculated O−H bond length of the silanol in free form was detected to be slightly shorter than that in the complex. This fact is true for all calculated methods and basis sets used. However, such a change was not clearly observed for the O−H bond length and the H−O−H angle of the water molecule.

Vibrational Frequencies of Single Silanol Complexes. In terms of vibrational frequency, the calculated data were summarized in Table 4. The two symmetrical O−H stretchings of the free water molecule yielded from the B3LYP calculations (3648 and 3654 cm^{-1}) are in excellent agreement with the value 3657 cm^{-1} obtained experimentally for the gas phase frequency.[19] The HF values 3732 and 3731 cm^{-1} are 75 cm^{-1} higher than the experimental data. The above finding leads to

TABLE 3: Bond Length and Bond Angle of Water, Naked Surface, and Complex between Water and Single Silanol Group (Figure 2) Using Different Methods of Calculation Where the Subscripts "s" and "w" Stand for Surface and Water Molecules, Respectively[a]

structure	method	$r(O_s-H_s)$ (Å)	$r(O_s\cdots O_w)$ (Å)	$r(O_w-H_w)$ (Å)	$\angle H_w-O_w-H_w$ (deg)
			Water		
exptl	ref 19			0.9576	104.48
calcd	HF/6-31G(d,p)			0.9431	106.04
	B3LYP/6-31G(d,p)			0.9653	103.71
	HF/6-31++G(d,p)			0.9433	107.12
	B3LYP/6-31++G(d,p)			**0.9652**	**105.73**
			Naked Surface		
calcd	HF/6-31G(d,p)	0.9396			
	B3LYP/6-31G(d,p)	0.9600			
	HF/6-31++G(d,p)	0.9399			
	B3LYP/6-31++G(d,p)	**0.9599**			
			Complex		
exptl	ref 20	0.956−1.000	2.70−2.90		
calcd					
single-I	HF/6-31G(d,p)	0.9494	2.8477	0.9434	107.45
	B3LYP/6-31G(d,p)	0.9758	2.7464	0.9640	106.56
	HF/6-31++G(d,p)	0.9485	2.8883	0.9441	107.87
	B3LYP/6-31++G(d,p)	**0.9736**	**2.7958**	**0.9651**	**107.34**
single-II	HF/6-31G(d,p)	0.9417	2.9459	0.9442	107.40
	B3LYP/6-31G(d,p)	0.9620	2.8933	0.9675	105.87
	HF/6-31++G(d,p)	0.9422	2.9405	0.9445	107.97
	B3LYP/6-31++G(d,p)	**0.9623**	**2.8772**	**0.9679**	**106.91**
single-III	HF/6-31G(d,p)	0.9438	2.8900	0.9428	106.34
	B3LYP/6-31G(d,p)	0.9651	2.7200	0.9646	104.67
	HF/6-31++G(d,p)	0.9439	2.9470	0.9432	107.17
	B3LYP/6-31++G(d,p)	**0.9649**	**2.8090**	**0.9652**	**106.03**

[a] The B3LYP/6-31++G(d,p) data (in bold font) were proposed to be the optimal values.

TABLE 4: Vibrational Frequencies of Water, Naked Surface, and Complex between Water and Single Silanol Group (Figure 2) Using Different Methods of Calculation Where ν_s, ν_1, ν_2, and δ Are Silanol−OH Stretching, Water Symmetric Stretching, Water Asymmetric Stretching, and Water Bending, Respectively[a]

structure	method	ν_s (cm^{-1})	ν_1 (cm^{-1})	ν_2 (cm^{-1})	δ (cm^{-1})
			Water		
exptl	ref 19		3657	3756	1595
calcd	HF/6−31G(d,p)		3732	3795	1574
	B3LYP/6−31G(d,p)		3648	3756	1599
	HF/6−31++G(d,p)		3731	3798	1538
	B3LYP/6−31++G(d,p)		**3654**	**3772**	**1536**
			Naked Surface		
exptl	ref 10	3650−3800			
calcd	HF/6−31G(d,p)	3834			
	B3LYP/6−31G(d,p)	3781			
	HF/6−31++G(d,p)	3833			
	B3LYP/6−31++G(d,p)	**3788**			
			Complex		
calcd					
single-I	HF/6−31G(d,p)	3664	3734	3797	1566
	B3LYP/6−31G(d,p)	3489	3670	3783	1571
	HF/6−31++G(d,p)	3681	3726	3789	1551
	B3LYP/6−31++G(d,p)	**3531**	**3663**	**3777**	**1551**
single-II	HF/6−31G(d,p)	3807	3713	3779	1575
	B3LYP/6−31G(d,p)	3757	3605	3719	1587
	HF/6−31++G(d,p)	3804	3707	3775	1554
	B3LYP/6−31++G(d,p)	**3759**	**3596**	**3717**	**1549**
single-III	HF/6−31G(d,p)	3786	3738	3801	1564
	B3LYP/6−31G(d,p)	3722	3659	3770	1576
	HF/6−31++G(d,p)	3783	3735	3800	1535
	B3LYP/6−31++G(d,p)	**3728**	**3659**	**3774**	**1532**

[a] The B3LYP/6-31++G(d,p) data (in bold font) were proposed to be the optimal values.

the clear conclusion that the B3LYP method is appropriate not only for the geometry optimization but also for reproducing the experimental frequency.

For the naked surface, the experimental symmetric OH stretchings (Table 4) determined from the silica and siliceous surfaces are in a broad range (3650−3800 cm^{-1}),[10] and that of the silicalite-1 surface is not available. On the basis of the evidence detected for pure water where the B3LYP/6-31++G-(d,p) calculated frequency is in excellent agreement with the experimental one, it can be, therefore, suggested that the predicted O−H stretching of the silanol group on the naked surface of the silicalite-1 is ∼3790 cm^{-1}. Note that there is no
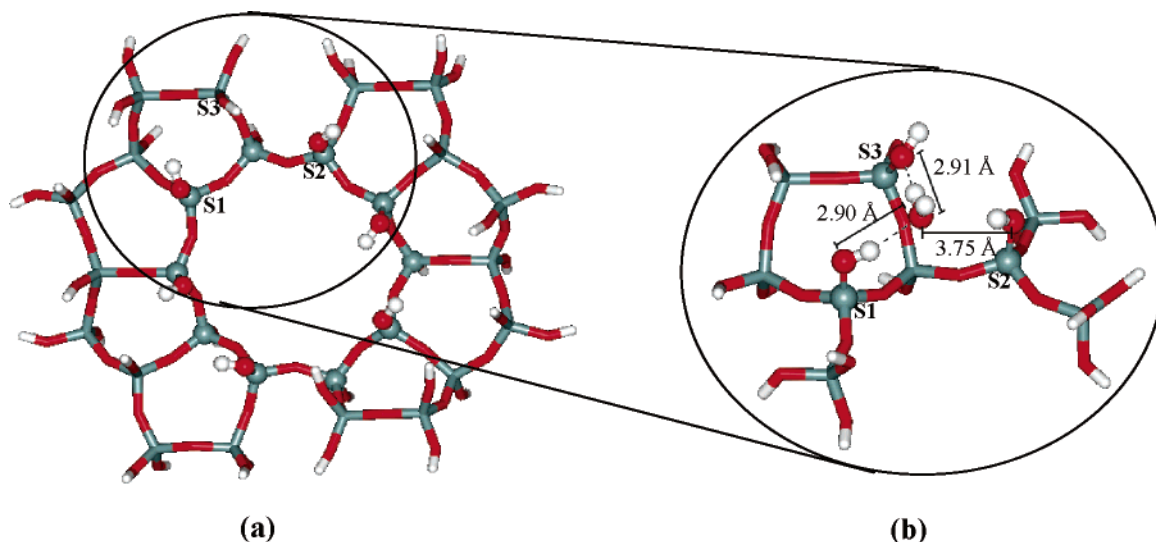
Figure 4. (a) The (010) surface of silicalite-1 and (b) with the initial configuration shown in Figure 3d, the B3LYP/6-31++G(d,p) fully optimization procedure brings the water molecule to the new configuration where the water molecule prefers to coordinate to S3 (see Figure 1d) rather than to S2.

significant difference in the vibrational frequencies arising from the same method using different basis sets.

Compared to the most stable single-I configuration, the complexation leads to a red shift of the symmetric O−H stretching of the silanol group by approximately 150−170 and 260−290 cm^{-1} for the HF and B3LYP calculations, respectively. This event was, somehow, not detected for the O−H bond of the water molecule.

A very similar behavior was observed for the asymmetric stretching (Table 4), and the bending mode of vibration of the water molecule which is reproduced by (i) the B3LYP method is more accurate than the HF one in comparison to the experimental data. (ii) there is no difference between the results due to the different basis sets used and (iii) complexation does not lead to significant changes of the three vibrational frequencies of the water molecule. An exception was found for the bending mode where the value 1536 cm^{-1} obtained from the bigger basis set, 6-31++G(d,p), in the B3LYP calculation is less reliable than the value 1599 cm^{-1} yielded from the 6-31G-(d,p) basis set where the experimental value is 1595 cm^{-1}. This event was found for the bending modes of both free water and its complex. The description can be due to the diffusivity nature of the 6-31++G(d,p) basis set where the interaction is slightly too repulsive when the two hydrogen atoms of the water molecule move close to each other, and vice versa. Clarification was made using the MP2 calculation for the water molecule. It is known that, with this method, the electron correlation was included. The MP2/6-31G(d,p) and MP2/6-31++G(d,p) calculations give bending frequencies of 1598 and 1532 cm^{-1}, respectively. These results confirm the above description on the greater reliability of the 6-31G(d,p) basis set as compared with the 6-31++G(d,p) basis set in the prediction of the bending mode of the molecule.

Double Silanol Complexes. For the sake of accuracy, as stated in the case of single-I, only the B3LYP/6-31++G(d,p)//B3LYP/6-31++G(d,p) calculations were applied to investigate interaction and optimal configuration between water and the two nearest silanol groups (Figure 3). The optimal values are summarized in Table 5. Note that the binding between two silanols and one water molecule requires an additional step in rotating of the silanol groups to the configuration suitable for complexation. The rotational energy was included in the ΔE_{def}

TABLE 5: Deformation Energy and Binding Energy (kJ/mol) Representing the Interaction between Water and Two Silanol Groups in the Configurations Shown in Figure 3 Where the Surface Optimization and the Energy Calculations Were Performed Using B3LYP/6-31++G(d,p) (See Calculation Details)

cluster type	ΔE_{def}	ΔE_{int}	ΔE_{bind}
double-near-I	34.94	−50.70	−15.76
double-near-II	23.74	−13.42	10.32
double-near-III	9.53	−35.15	−25.62
double-far-I*	2.59	−51.41	−48.82
double-far-II	1.05	−75.87	−74.82 (−37.41)

^{a} With the initial configuration shown in Figure 3d, the optimal structure in Figure 4b was yielded.

value of the cluster, defined in eq 2a, which was added to the interaction energy in eq 1.

Some comments should be made concerning the final geometry of the double-far-I complex. With the initial configuration shown in Figure 3d, the B3LYP/6-31++G(d,p) fully optimization procedure brings the water molecule to the configuration shown in Figure 4b where the water molecule prefers to coordinate to S3 (see Figure 1d) rather than to S2. Here, the distance from the O atom of water to the O atom of silanol S1 or S3 is 2.90 Å, while that of S2 is 3.75 Å. This result supports our assumption made in section 2 (calculation details) that the distance between the two silanols, S1 and S2, in the double-far is too large for a single water molecule to form hydrogen bonds with both silanols.

In terms of complex stability, the most stable complex takes place via the double-far-I complex. The corresponding binding energy is −48.82 kJ/mol. This value is significantly lower than the values −37.41 kJ/mol for the double-far-II complex and −25.62 kJ/mol for the double-near-III complex. In addition, the deformation energies for the double silanol complexes shown in Table 5 are higher than those of the single silanol in Table 2 due to the addition of the rotational energy into the ΔE_{def} term, as defined in eq 2a.

The rotational energy for the double-far configurations is much lower than that of the double-near complexes due to a larger O−O distance between the two silanols which amounts to 5.75 and 3.86 Å, respectively. The strong repulsion between the two OH groups leads to a ΔE_{def} value in the double-near-I configuration (Figure 3a) of 34.94 kJ/mol. This energy decreases

Saengsawang et al.

to 23.74 kJ/mol when the two OH groups turn away from each other (double-near-II, Figure 3b). In addition, the repulsion is lower when the H atom of one OH group points toward the O atom of the other OH group (Figure 3c). Note that the strong repulsion between the two silanol groups is partially due to an artifact of the cluster approach where a periodic crystal structure is not taken into consideration. However, the same assumption was applied for all models. Therefore, the comparison should not be influenced remarkably by this effect and the trend will remain unchanged.

Taking into account all the data summarized above, the B3LYP/6-31++G(d,p) binding energies are in the following order: double-far-I < double-far-II ∼ single-I ∼ single-IV ∼ double-near-III. Since the stability of −48.82 kJ/mol for the double-far-I complex (Figure 3d) is significantly lower than those for the other configurations, these areas on the (010) surface of the silicalite-1 are supposed to be the first binding sites which have to be covered when the water molecule approaches the surface. In other words, the most stable conformation takes place when a water molecule forms two hydrogen bonds with two silanols, with only one lying on the opening pore of the straight channel. When the water loading increases, the next favorable silanols are those of the opening pore in which the complex conformations are double-far-II, single-I, single-IV, and double-near-III.

References and Notes

(1) Chandress, M.; Webb, E. B., III; Grest, G. S.; Martin, M. G.; Thompson, A. P. *J. Phys. Chem. B* **2001**, *105*, 5700.

(2) Pieterse, J. A. Z.; Veefkind-Reyes, S.; Seshan, K.; Lercher, J. A. *J. Phys. Chem. B* **2000**, *104*, 5715.

(3) Tanaka, H.; Zheng, S.; Jentys, A.; Lercher, J. A. *Stud. Surf. Sci. Catal.* **2002**, *142*, 1619.

(4) Turro, N. J. *Acc. Chem. Res.* **2000**, *33*, 637.

(5) Turro, N. J.; Lei, X.; Li, W.; Liu, Z.; Ottaviani, M. F. *J. Am. Chem. Soc.* **2000**, *122*, 12571.

(6) Park, S. H.; Rhee, H. K. *Catal. Today* **2000**, *63*, 267.

(7) Klemm, E.; Scheidat, H.; Emig, G. *Chem. Eng. Sci.* **1997**, *52*, 2757.

(8) Aguilar, J.; Corma, A.; Melo, F. V.; Sastre, E. *Catal. Today* **2000**, *55*, 255.

(9) Denoyer, J. F.; Baron, G. V.; Vanbutsele, G.; Jacobs, P. A.; Martens, J. H. *Chem. Eng. Sci.* **1999**, *54*, 3553.

(10) Zecchina, A.; Bordiga, S.; Spoto, G.; Marchese, L. *J. Phys. Chem.* **1992**, *96*, 4991.

(11) Trombetta, M.; Busca, G.; Lenarda, M.; Storaro, L.; Pavan, M. *Appl. Catal., A* **1999**, *182*, 225.

(12) Armaroli, T.; Bevilacqua, M.; Trombetta, M.; Milella, F.; Alejandre, A. G.; Ramírez, J.; Notari, B.; Willey, R. J.; Busca, G. *Appl. Catal., A* **2001**, *216*, 59.

(13) Trombetta, M.; Armaroli, T.; Alejandre, A. G.; Solis, J. R.; Busca, G. *Appl. Catal., A* **2000**, *192*, 125.

(14) Armaroli, T.; Trombetta, M.; Alejandre, A. G.; Solis, J. R.; Busca, G. *Chem. Phys.* **2000**, *2*, 3341.

(15) Kawai, T.; Tsutsumi, K. *Colloid Polym. Sci.* **1998**, *276*, 992.

(16) Olson, D. H.; Haag, W. O.; Borghard, W. S. *Microporous Mesoporous Mater.* **2000**, *35*, 435.

(17) Trombetta, M.; Busca, G. *J. Catal.* **1999**, *187*, 521.

(18) Frisch, M. J.; Trucks, G. W.; Schlegel, H. G.; Scuseria, G. E.; Robb, M. A.; Cheeseman, J. R.; Zakrzewski, V. G.; Montgomery, J. A., Jr.; Stratmann, R. E.; Burant, J. C.; Dapprich, S.; Millam, J. M.; Daniels, A. D.; Kudin, K. N.; Strain, M. C.; Farkas, O.; Tomasi, J.; Barone, V.; Cossi, M.; Cammi, R.; Mennucci, B.; Pomelli, C.; Adamo, C.; Clifford, S.; Ochterski, J.; Petersson, G. A.; Ayala, P. Y.; Cui, Q.; Morokuma, K.; Salvador, P.; Dannenberg, J. J.; Malick, D. K.; Rabuck, A. D.; Raghavachari, K.; Foresman, J. B.; Cioslowski, J.; Ortiz, J. V.; Baboul, A. G.; Stefanov, B. B.; Liu, G.; Liashenko, A.; Piskorz, P.; Komaromi, I.; Gomperts, R.; Martin, R. L.; Fox, D. J.; Keith, T.; Al-Laham, M. A.; Peng, C. Y.; Nanayakkara, A.; Challacombe, M.; Gill, P. M. W.; Johnson, B.; Chen, W.; Wong, M. W.; Andres, J. L.; Gonzalez, C.; Head-Gordon, M.; Replogle, E. S.; Pople, J. A. *Gaussian 98*, revision A.11; Gaussian Inc.: Pittsburgh, PA, 2001.

(19) Eisenberg, D.; Kauzmann, W. *The Structure and Properties of Water*; Oxford University Press: Oxford, U.K., 1969.

(20) Nyfeler, D.; Armbruster, T. *Am. Mineral.* **1998**, *83*, 119.